Optical constants of single-crystalline Ni(100) from 77 to 770 K from ellipsometry measurements

(iD) **Farzin Abadizaman, Jaden Love and** (iD) **Stefan Zollner**

View Online   Export Citation   CrossMark
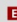
Optical constants of single-crystalline Ni(100) from 77 to 770 K from ellipsometry measurements

Farzin Abadizaman,[1,a)] (iD) Jaden Love,[2,b)] and Stefan Zollner[2,c)] (iD)

AFFILIATIONS

[1] Department of Condensed Matter Physics, Faculty of Science, Masaryk University, Kotlářská 2, 611 37 Brno, Czech Republic
[2] Department of Physics, New Mexico State University, P.O. Box 30001, Las Cruces, New Mexico 88003

[a)] Author to whom correspondence should be addressed: abadizaman@physics.muni.cz
[b)] Email: lovej@nmsu.edu
[c)] Email: zollner@nmsu.edu. URL: http://ellipsometry.nmsu.edu

ABSTRACT

Ellipsometry measurements were taken on single-crystalline Ni(100) at various temperatures between 77 and 770 K. DC conductivity and resistivity are extracted from the model optical constants and their temperature dependence is discussed. The authors find only qualitative agreement in the general trend of the resistivity measured by ellipsometry and electrical measurements. The temperature dependence of the main absorption peak at 4.8 eV indicates that the interband transitions are scattered by magnons with an effective energy of about 53 meV. The width of the main absorption peak reduces by 0.38 eV as the temperature rises, which is interpreted as the ferromagnetic exchange energy at the L-point. The small absorption peak at 1.5 eV is prominent only in the ferromagnetic phase and almost disappears in the paramagnetic phase. This peculiarity is explained by assigning the peak to $K_{3\downarrow} \rightarrow K_{2\downarrow}$ transitions, which accounts for the decrease of the magnitude of the peak and its constant energy.

Published under an exclusive license by the AVS. https://doi.org/10.1116/6.0001763

I. INTRODUCTION

This paper is an extension of our previous article,[1] hereafter referred to as I, where we modeled the dielectric function of bulk polycrystalline Ni from ellipsometry measurements in an energy range of 0.06–6 eV at 300 K. The model consists of two Drude and five Lorentzian oscillators to describe the two carrier types (s- and d-electrons) and interband transitions. In this work, we model the dielectric function of single-crystalline Ni(100) at temperatures from 77 to 770 K with temperature steps of about 50 K. The temperature dependence of interband transitions sheds light on the origin of the absorption peaks in the optical conductivity.

Nickel has been extensively studied theoretically and experimentally, for instance, in Refs. 2–9 and references therein. It is a ferromagnetic metal with a face centered cubic crystal structure, a Curie temperature of 627 K, and a very high DC conductivity of $138 \times 10^3 \, (\Omega \, \text{cm})^{-1}$ at room temperature.[10] The easy magnetic direction of Ni is $\langle 111 \rangle$ with a saturation magnetization of 485 (emu/cm³) at 290 K and the saturation magnetic moment of $0.606 \, \mu_B$/atom,[11] where μ_B is the Bohr magneton. This paper is inspired by the work

of Shiga and Pells[12] and Kirillova *et al.*[13] who studied the temperature dependence of the optical properties of polycrystalline and single-crystalline Ni(110), respectively. The purpose of this work is to investigate the discrepancies that are observed in the description of the temperature dependence of the energy of the main peak at 4.8 eV and the origin of the small peak at 1.5 eV. Shiga and Pells describe the red shift of the main absorption peak in the optical conductivity as a linear shift. In this work, we fit the red shift with a Bose–Einstein model,[14] and further discussion about the interband transitions is provided. In addition, the temperature dependence of the absorption peak at 1.5 eV is studied using the change of optical conductivity[15] $\delta\sigma = \sigma(T) - \sigma(770)$. This method reveals a significant feature of this peak that has not been observed before due to being buried under the large plasma frequencies of Ni. This method also provides new insight into the origin of the absorption peak at this energy.

II. EXPERIMENTAL RESULTS AND DATA ANALYSIS

The measurements were taken on a $10 \times 10 \, \text{mm}^2$ single-crystalline Ni(100) sample with a thickness of 0.5 mm and purity
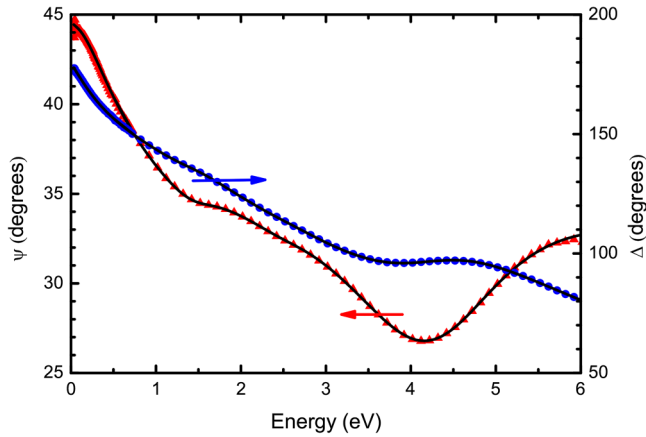
FIG. 1. Ellipsometric angles ψ (▲) and Δ (●) of clean single-crystalline Ni(100) at 300 K at an angle of incidence of 70°. Symbols show experimental data, lines the best fit with Eq. (1), and parameters are shown in Table I. Not all data points are shown.

of >99.99%, which was obtained commercially.[16] The surface roughness of the sample was determined by atomic force microscopy to be about 2 nm. The cleaning procedure and experimental setup are described in I. After heat treating the sample in a UHV cryostat at 770 K and at a pressure of 10^{-7} Torr, ellipsometry measurements at an angle of incidence of 70° were taken with a J. A. Woollam VASE ellipsometer from 0.5 to 6.5 eV with a step size of 20 meV from 770 to 77 K in 50 K steps. The sample was kept at each temperature for 30–45 min to reach thermal equilibrium. Afterward, the same measurements were taken in reverse order from 77 to 770 K. No significant changes in the data at the same temperatures in the two runs of increasing and decreasing temperature were observed. Next, the sample was mounted in another UHV cryostat with diamond view ports and was heat treated at 770 K to remove possible contamination and oxidation from transferring the sample from one instrument to the other. The same ellipsometry measurements were then taken with a J. A. Woollam FTIR ellipsometer from 0.03 to 0.8 eV with a resolution of 16 cm^{-1}. The data from the two instruments were merged using the window correction procedure described elsewhere.[17] More experimental details are described in a recent review article.[18]

Two Drude and four Lorentzian oscillators were used to model the dielectric function of Ni. This model has one Lorentzian oscillator less than in I because the merging procedure removes the mismatch between the data from the two instruments and reduces the minimum number of oscillators needed to model the dielectric function, which is given by six oscillators with a total of 16 parameters to fit[1]

$$\epsilon(E) = 1 + \sum_{i=1}^{2} \frac{-E_{p,i}^2}{E(E + i\gamma_i)} + \sum_{i=1}^{4} \frac{A_i E_{0,i}^2}{E_{0,i}^2 - E^2 - i\gamma_i E}. \quad (1)$$

Figure 1 demonstrates the measured ellipsometric angles of cleaned single-crystalline Ni(100) for a 70° angle of incidence at 300 K modeled by Eq. (1) with the parameters given in Table I. To reduce the number of correlated parameters, the energy of the first Lorentzian oscillator at about 1.5 eV is retained constant as explained later in this work and also suggested in other studies.[12] Furthermore, the broadening of the Lorentzian oscillator at about 12 eV is retained constant since it is beyond our spectral range. All data were corrected for 20 Å of surface roughness using the Bruggeman effective medium approximation.[19] As Table I shows, the third Lorentz oscillator at 4.77 eV is the strongest among other ones so we refer to it as the main peak and the first Lorentz oscillator at 1.57 eV as the small absorption peak throughout this work. The second Lorentz oscillator at 2.58 eV is very weak. However, it is needed to achieve a good model. The fourth Lorentz oscillator at 12.7 eV is located at a very high energy with very large broadening to describe the absorption that occurs above our spectral range. Just like in the original work of Drude,[20–22] we are using two Drude terms. It is debatable whether these Drude terms represent two physically distinct carrier species or a frequency dependence of the scattering rate of a single species of carriers.[1] For this work, we consider Drude 1 to be d-electrons and Drude 2 to be s-electrons. This will be further explained in Sec. III.

III. OPTICAL CONDUCTIVITY

Figure 2 shows the real and imaginary parts of the optical conductivity of our Ni sample at various temperatures. Two well known features at about 1.5 and 4.8 eV are present in the real part.[12,20,23,24] The peak at about 1.5 eV is mainly due to the transitions within the minority spin bands (spin down), whereas both spin directions contribute to the main peak at 4.8 eV, which is

TABLE I. Parameters used to describe the optical constants of single-crystalline Ni(100) at T = 300 K: A is the amplitude, E_p is the plasma energy, E_0 is the energy, and γ is the broadening. The DC conductivity σ_0 was calculated from the Drude parameters using Eq. (2). The parameter marked (f) was fixed during the fit.

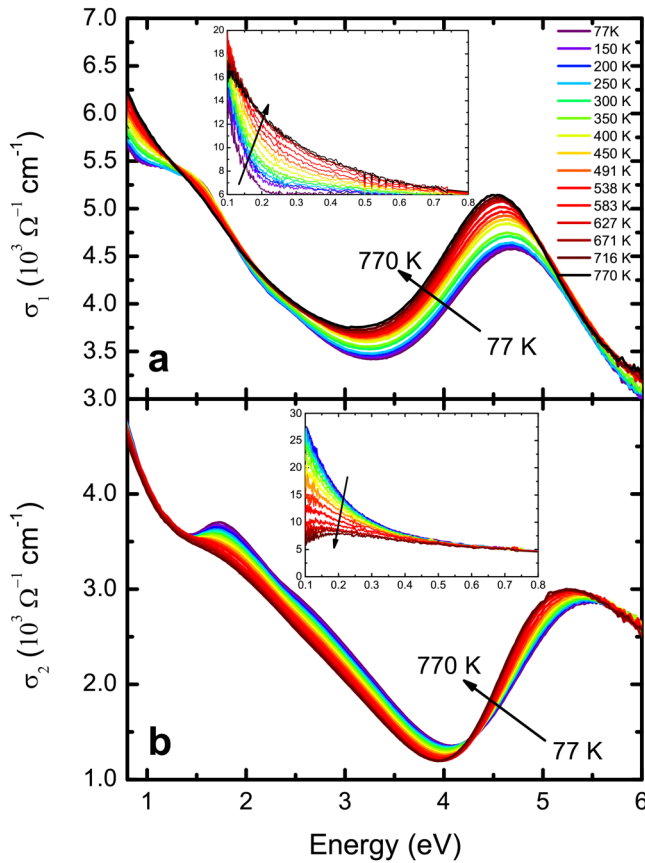|	A (1)	E_P (eV)	E_0 (eV)	γ (eV)	σ_0 (1/Ωcm)
Drude 1 (d)		12.09 ± 0.05		2.91 ± 0.02	6,766
Drude 2 (s)		4.806 ± 0.004		0.0403 ± 0.0003	77,200
Lorentz 1	1.83 ± 0.07		1.565 ± 0.006	0.847 ± 0.027	
Lorentz 2	0.138 ± 0.033		2.584 ± 0.017	0.888 ± 0.11	
Lorentz 3	2.419 ± 0.024		4.769 ± 0.002	2.084 ± 0.01	
Lorentz 4	1.905 ± 0.006		12.65 ± 0.098	6.01 (f)	

FIG. 2. Real (a) and imaginary (b) parts of the optical conductivity of single-crystalline Ni(100) from 77 to 770 K. The insets show the infrared spectral range. The arrows indicate the direction of rising temperature. The data below 0.1 and above 6.0 eV are not shown due to noise.
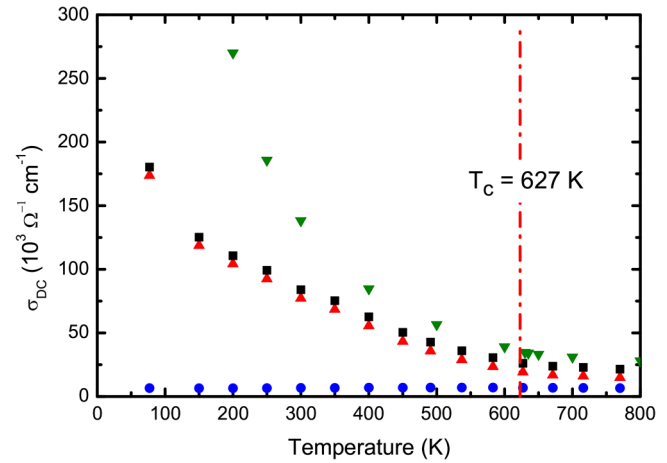

FIG. 3. DC conductivity of Ni obtained from ellipsometry measurements. Total DC conductivity (■), DC conductivity of s-electrons (▲), DC conductivity of d-electrons (●), and DC conductivity from electrical measurements 10 (▼). Most of the conductivity of Ni below T_c is due to s-electrons. IR spectroscopic ellipsometry underestimates σ_{DC}.

dominated by transitions from the bottom of the d-band to the states near the Fermi level.[25] The temperature dependence of optical properties of Ni has been little investigated. Johnson and Christy[26] claim that the optical constants of Ni do not change over the temperature range between 77 and 423 K and that they are identical to their optical constants at room temperature. However, Fig. 2 displays a noticeable change in the optical constants of Ni as the temperature rises. Such changes have also been reported by Shiga and Pells.[12] Many interband transitions have been assigned to the absorption peaks based on the calculated or experimental band structures.[12,23,27] Using polarimetry techniques, Stoll[27] has reported several small interband transition peaks in the optical conductivity of ferromagnetic and paramagnetic single-crystalline Ni (110) at various temperatures. We do not observe any of those peaks in the optical conductivity of our sample. Stoll's measurements on polycrystalline Ni[23] also show many small structures between 2.0 and 2.5 eV, which are not observed in our data. Stoll and Jung[28] suggest that the free carrier part of the imaginary part of the dielectric function (Drude term) increases with temperature

as a function of T^2. Our measured data also indicate an increase below 0.8 eV as the temperature rises. However, Fig. 2 illustrates that the Drude term increases with temperature up to about the Curie temperature T_c and stays almost constant above that. Another noticeable feature in Fig. 2 is the change in the magnitude of the small peak at 1.5 eV in the transition from ferromagnetic to paramagnetic phase. To the best of our knowledge, this has not been reported in the literature thus far. We will discuss this matter further in Sec. VI.

The DC conductivity can be found as the zero energy limit of the Drude response,[1]

$$\sigma_{DC} = \frac{\epsilon_0}{\hbar}\frac{E_p^2}{\gamma}. \quad (2)$$

If there are more than one carrier species, the DC conductivity is defined as[29]

$$\sigma_{DC,total} = \sum_{i=1}^{n}\sigma_{DC,i}. \quad (3)$$

Figure 3 shows the contribution of the first and the second Drude terms to the total DC conductivity of Ni(100) from Eqs. (2) and (3). As the figure shows, the first Drude term does not contribute significantly to the total DC conductivity below T_c, whereas the contribution from the second Drude term demonstrates a typical metallic behavior as the temperature increases. This behavior can also be seen in the temperature dependence of the scattering rates of the two Drude terms in Eq. (1) shown in Fig. 4. This figure shows that the scattering rate of the first Drude term is very large and does not change significantly with temperature, which is expected for the highly localized d-electrons,
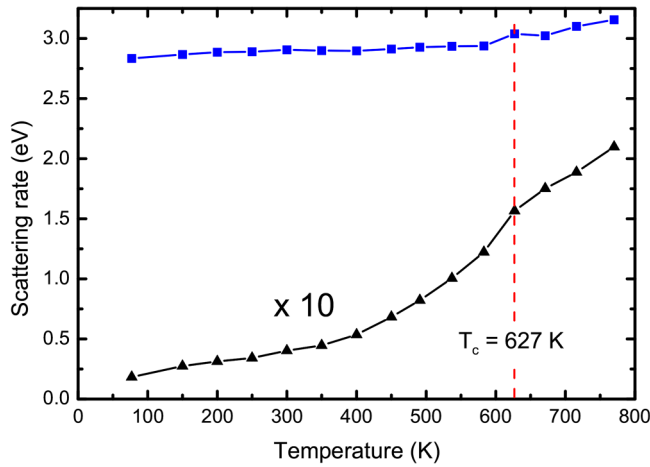
FIG. 4. Scattering rates of the first (■) and second (▲) Drude terms in Eq. (1) as a function of temperature. For clarity, the broadening of the second Drude term (s-electrons) is multiplied by 10.

FIG. 5. Extrapolated optical conductivity of single-crystalline Ni (100) between 77 and 770 K. The arrow shows the direction of rising temperature.

whereas the scattering of the second Drude term is an order of magnitude smaller and increases by a factor of about 9 as the temperature rises, thus attributing these terms to d- and s-electrons, respectively. The change in the slope of the scattering rate of s-electrons around the Curie temperature is due to the different scattering mechanism in the ferromagnetic and paramagnetic phases.[2] In the paramagnetic phase, s-electrons with both spin states can scatter into the d-band, whereas in the ferromagnetic phase, only half of the s-electrons can scatter into d-bands since half of the d-band is completely full, which decreases the scattering rate of the s-electrons drastically.[2]

The plasma frequencies of s- and d-electrons also vary with temperature. However, since the plasma frequencies are fitting parameters and are correlated, and also considering the uncertainty of effective masses and their variation across the Brillouin zone,[7] it is difficult to interpret the change of the plasma frequencies with temperature. We only state that for the s-electrons we find $E_p^2 = 23 \pm 1$ eV^2. Assuming $m^* = 1.4$ for s-electrons[24] yields 0.25 electrons per atom, which is reasonable.[24] For the d-electrons, E_p^2 varies from 140 eV^2 at low temperatures to 155 eV^2 at high temperatures. Assuming $m^* = 3$, we find 3.6 d-electrons per atom near the Fermi surface, which is an order of magnitude larger than the reported value.[24] This discrepancy is likely due to the uncertainty of the effective mass used in this calculation. Comparison of DC conductivity taken from ellipsometry measurements to electrical measurements shows that IR spectroscopic ellipsometry underestimates the DC conductivity. This is due to the fact that our ellipsometer measures down to 0.1 eV for measurements on our sample inside the cryostat without too much noise. Below this energy, one has to extrapolate the model to obtain DC conductivity. Figure 5 shows the optical conductivity extrapolated down to zero. As the figure shows, the difference in the optical conductivity at various temperatures becomes more significant at the energies below 0.06 eV, which is below our spectral range.
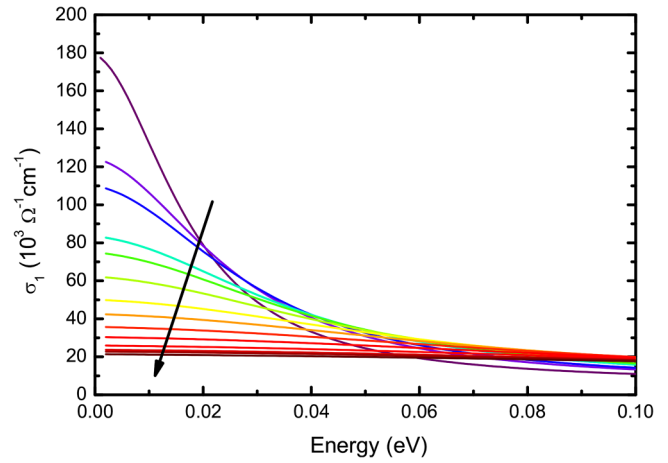
The Drude behavior for a single carrier type can be written as[29]

$$\epsilon^D(E) = -\frac{E_p^2}{E^2 + i\gamma E} = -\frac{E_p^2}{E^2 + \gamma^2} + i\frac{E_p^2\gamma}{E(E^2 + \gamma^2)}, \quad (4)$$

which yields

$$\epsilon_1^D(E) = -\frac{1}{\gamma}(E\epsilon_2^D). \quad (5)$$

This relation is applicable well below the onset of the interband absorption edge, where only free carrier absorption is present. According to Eq. (5), plotting ϵ_1 against $E\epsilon_2$ should be linear and the slope should be equal to $-1/\gamma$. Figure 6 shows ϵ_1 vs $E\epsilon_2$ of Ni at various temperatures. Fitting a line in the linear region of Fig. 6 ($\epsilon_2 E > 50$ eV), we calculated the scattering rate in Eq. (5). We find good agreement between this scattering rate and the scattering rate of s-electrons in Eq. (1) as demonstrated in Fig. 7.

It has been suggested[30] that the deviation from linearity indicates the onset of interband absorption. From Fig. 6, it is found that deviation from linearity occurs at about 0.5 eV and varies with temperature. However, it has been shown[31,32] that the onset of interband absorption in Ni occurs at about 0.15 eV and is independent of temperature. The reason for this discrepancy might be the fact that there are two Drude terms in the dielectric function of Ni. Assuming two Drude terms, Eq. (4) becomes

$$\epsilon^D(E) = -\frac{E_{p1}^2}{E^2 + i\gamma_{D1}E} - \frac{E_{p2}^2}{E^2 + i\gamma_{D2}E}, \quad (6)$$
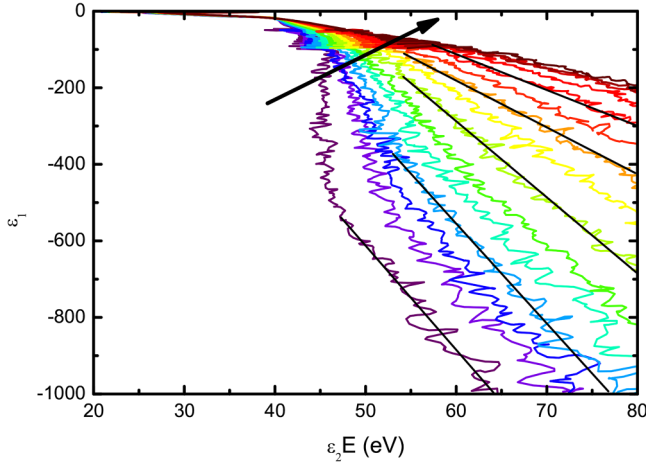
FIG. 6. ϵ_1 vs $E\epsilon_2$ for single-crystalline Ni(100). Solid lines show the fitted line to the linear part at selected temperatures.

which yields

$$\epsilon_1^D(E) = \frac{E_{p1}^2(E^2 + \gamma_{D2}^2) + E_{p2}^2(E^2 + \gamma_{D1}^2)}{E_{p1}^2\gamma_{D1}(E^2 + \gamma_{D2}^2) + E_{p2}^2\gamma_{D2}(E^2 + \gamma_{D1}^2)}(E\epsilon_2^D). \quad (7)$$

Due to the large value of the scattering rate of the first Drude term from Table I at 300 K ($\gamma_{D1} = 2.91\,eV$), Eq. (7) is linear only well above the onset of interband absorption, where $(\gamma_{D1}/E)^2$ becomes negligible. Therefore, it appears that this method cannot be used to find the onset of interband transitions of transition metals.
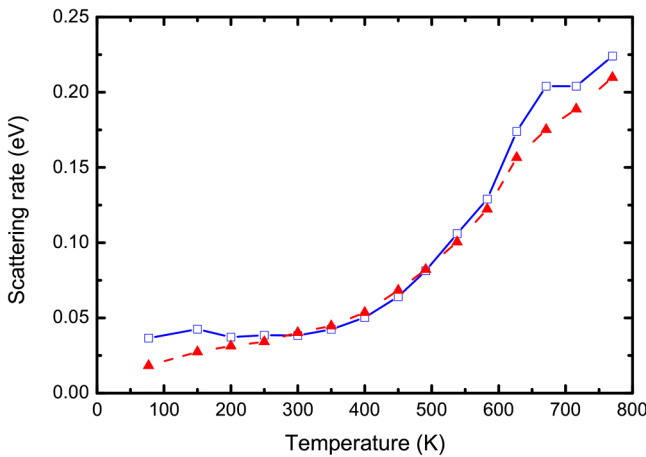

FIG. 7. Scattering rate obtained from Eq. (5) (□), and the scattering rate of the second Drude term (s-electrons) in Eq. (1) (▲) at various temperatures.

IV. RESISTIVITY

The resistivity of Ni is governed by scattering of free electrons by impurities (ρ_{imp}), lattice vibrations (ρ_{e-ph}), other electrons (ρ_{e-e}), and magnons (ρ_{e-mag}). According to Matthiessen's rule, the total resistivity of Ni may be written as a sum of these terms,[33]

$$\rho_{total} = \rho_{imp} + \rho_{e-e} + \rho_{e-ph} + \rho_{e-mag}. \quad (8)$$

The first term in Eq. (8) is the residual resistivity and can be neglected only for highly pure metals.[34] However, there are two more contributions in the residual resistivity of ferromagnets, namely, magnetostriction and magnetocrystal residual resistance,[34] which cannot be ignored even for highly pure samples.

The electron-electron scattering term is called the Baber interaction[6] and takes into account the electron-electron and electron-hole scattering,

$$\rho_{e-e} = \frac{2m}{ne^2}\left(\frac{e^2}{2m}\right)^2\frac{m^3}{h^3}\left(\frac{kT}{\zeta_1}\right)^2\frac{e^\Delta(\pi^2 + \Delta^2)}{2(e^\Delta + 1)^2}H(\beta, q), \quad (9)$$

where e is the electronic charge, m is the effective mass of the light carrier, n is the electron density, k is the Boltzmann constant, h is Plank's constant, and ζ_1 is Fermi energy of the group of light carriers. $\Delta = \frac{m}{2kT}(u^2 - V_1^2)$, where u is the electron velocity and V_1 is the Fermi velocity. In the function $H(\beta, q)$, $\beta = m_2/m_1$ is the effective mass ratio of electrons in the final and initial states, and q is the screening factor that screens the field of a positive hole by a factor of e^{-qr}. Reference 6 provides numerical values of the function $H(\beta, q)$ for different effective mass ratios and screening factors. For sufficiently low temperatures where lattice vibrations can be neglected, Eq. (9) can be written as[6,34]

$$\rho_{e-e} = \frac{\pi^2 e^2 m^2}{16nh^3}\left(\frac{kT}{\zeta_1}\right)^2 H(\beta, q) = aT^2, \quad (10)$$

which shows that at low temperatures, the electron-electron interaction contributes to the temperature dependence of the resistivity as T^2. This term is negligible when β is unity as in the case of Cu[6] and is appreciable for Ni, where $\beta = m_d/m_s = 22$.[33] If there is only one type of carrier, electron-electron interaction contributes to the conductivity only when there is an electron-electron umklapp scattering process, whereas normal scattering does not contribute to the conductivity.[34] For more than one type of carriers, as in the case of Ni, the electron-electron scattering contributes to the conductivity according to Eq. (10) even if there is no umklapp process.[34]

Scattering of electrons by phonons may be written as[35]

$$\rho_{e-ph} = 4A\left(\frac{T}{\theta_D}\right)^5\int_0^{\theta_D/T}\frac{x^5}{(e^x - 1)(1 - e^{-x})}dx, \quad (11)$$

where A is a constant and θ_D is the Debye temperature. $\theta_D = 345\,K$ at $T = 293\,K$[36] and $\theta_D = 477\,K$ at $T = 0\,K$.[37] The resistivity $\rho_{e-ph} \propto T^5$ for T $\ll \theta_D$, and $\rho_{e-ph} \propto T$ for $T > \theta_D$. This temperature dependence is common in all metals. Another term that contributes to ρ_{e-ph} of transition metals is the reduction of the electron free path

due to the scattering of s-electrons into d-electron bands upon collision with phonons, which was proposed by Mott[2] and calculated by Wilson,[5]

$$\rho_{e-ph}^{sd} = d\left(\frac{T}{\theta_D}\right)^3 \int_{\theta_E/T}^{\theta_D/T} \frac{x^3}{(e^x - 1)(1 - e^{-x})} dx, \quad (12)$$

where d is a constant and $k\theta_E = h\nu_E$ is the minimum phonon energy required to excite s-d transitions. Equation (12) is proportional to T^3 and implies that s-d scattering is dominant at high temperatures. At sufficiently low temperatures, ρ_{e-ph} is dominated by the normal s-s and d-d transitions.[5]

The last factor contributing to the resistivity of Ni is the scattering of electrons by magnons. This scattering mechanism changes the direction of the spin of an electron[38] by annihilation or creation of magnons. The temperature dependence of the scattering between electrons and magnons in the range of $T_0 < T < 0.1T_c$, where spin wave approximation is applicable, is[34]

$$\rho_{e-mag}(T) \sim \exp\left(-\frac{T_0}{T}\right) \quad \text{at} \quad T \ll T_0, \quad (13)$$

$$\rho_{e-mag}(T) \sim T^2 \phi\left(\frac{T_0}{T}\right) \quad \text{at} \quad T \approx T_0, \quad (14)$$

$$\rho_{e-mag}(T) \sim T^2 \quad \text{at} \quad T \gg T_0, \quad (15)$$

where

$$\phi(t) = \frac{3}{2\pi^2} \int_t^\infty \frac{xe^x}{(e^x - 1)(x - 1)} dx. \quad (16)$$

T_0 is the frozen temperature, below which the electron-magnon scattering is non-effective. Goodings[39] calculated that below 10–20 K, the magnon assisted s-d scattering is negligible and ρ_{e-mag} is dominated by s-s scattering. He also found that at room temperature, ρ_{e-mag} due to s-d scattering is significantly greater than that of s-s scattering (about 130 times), and s-d scattering by two magnons, where the spin of the electron is unchanged, is two orders of magnitude smaller than s-d scattering by one magnon. Following Goodings's work, Raquet et al.[33,40] showed that 30% of the resistivity of Ni at room temperature is due to the spin-flip scattering via magnons, and an extremely large external magnetic field is needed to reduce the magnetic resistivity to zero. They found the frozen temperature T_0 to be $T_0 \approx 15$ K for $s^\pm$-$d^\mp$ scattering and $T_0 \approx 40$ K for $d^\pm$-$d^\mp$ scattering. By increasing T above T_c, the concentration of spin waves increases[11] and reaches its maximum; thus, a constant contribution to the resistivity is equal to[41]

$$\rho_{e-mag} = \frac{k_F(m\Gamma)^2}{4\pi e^2 Z\hbar^3} J(J + 1). \quad (17)$$

Here, J is the effective local spin, Γ is a coupling parameter, k_F is the Fermi wave vector, and Z is the atomic number.

Therefore, above T_c, the temperature dependence of the resistivity of Ni is proportional to T, in part due to the temperature
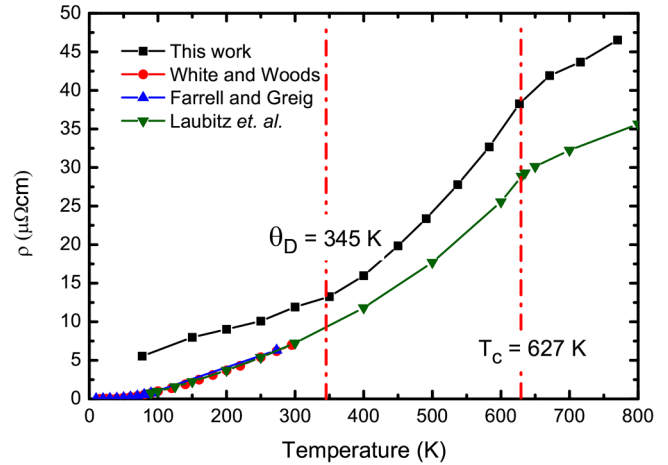

FIG. 8. Comparison of the optical resistivity ($\omega = 0$) of Ni from this work on (100) single-crystalline Ni (■) and electrical measurements on polycrystalline Ni by White and Woods (Ref. 35) (●), Ni rods from Farrell and Greig (Ref. 38) (▲), and polycrystalline rod by Laubitz et al. (Ref. 10) (▼).

dependence of electron-phonon scattering shown in Eq. (11).[42] However, the resistivity of Ni in the paramagnetic region is not entirely due to the electron-phonon scattering. Other scattering mechanisms, such as electron-electron scattering, also contribute to the resistivity.[10]

Figure 8 shows the resistivity of a single-crystalline Ni(100) from ellipsometry measurements (this work) and resistivity of polycrystalline Ni from electrical measurements by other authors.[10,35,38] The overall temperature dependence of the resistivity is only in qualitative agreement with Laubitz et al.[10] This is probably due to the different methods of measuring the resistivity. The resistivity taken from ellipsometry measurements is derived from an extrapolation of a model fitted to the ellipsometry data, whereas in electrical measurements the resistivity is measured directly. Another discrepancy that can be observed is the Curie temperature in our measurement, which appears to be slightly higher than the accepted Curie temperature of Ni, $T_c = 627$ K. This is probably due to a temperature gradient between the thermocouple and the sample.

Figure 9 shows $\log(\rho)$ vs $\log(T)$ and the fitted lines in selected regions. The resistivity shows a temperature dependence of T^2 between θ_D and T_c. In this temperature interval, both electron-phonon and electron-magnon interactions contribute to the resistivity of Ni. Although $\rho_{e-mag} \propto T^2$ at low temperatures, its temperature dependence is not a simple function of T at higher temperatures.[43] The stiffness of the spin waves decreases as the temperature rises and its value at T_c decreases to the order of a quarter of the room temperature value.[44] Therefore, it is not possible to separate the temperature dependence of ρ_{e-mag} and ρ_{e-ph} in this region. Figure 9 also shows that between 77 and 250 K, the temperature dependence is proportional to $\sqrt{T}$, which is not consistent with the temperature dependence of any individual contributions to the total resistivity. We believe that this discrepancy is due to the
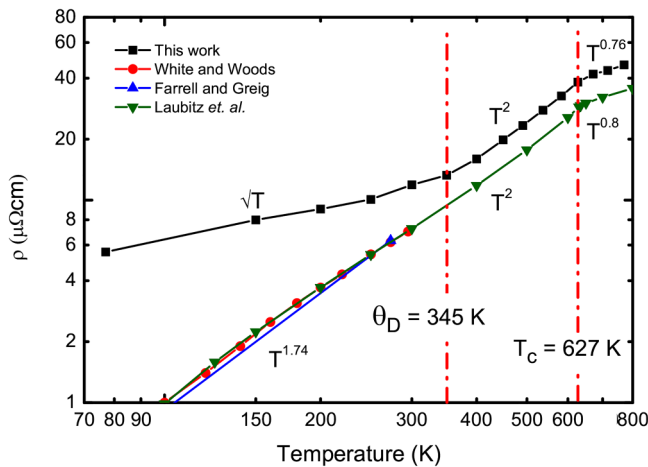
FIG. 9. Log-log plot of the resistivity of Ni at various temperatures from optical measurements (this work) and electrical measurements (Refs. 10, 35, and 38). A linear fit to the data from this work below room temperature shows a slope of 0.51 ± 0.02 and a slope of 1.97 ± 0.03 between Debye temperature θ_D and Curie temperature T_c, whereas a linear fit to the data from electrical measurements shows a constant slope of 1.74 ± 0.02 below Curie temperature T_c. A linear fit to the data above T_c shows a slope of 0.76 ± 0.07 and 0.80 ± 0.04 for this work and Laubitz et al. (Ref. 10), respectively.
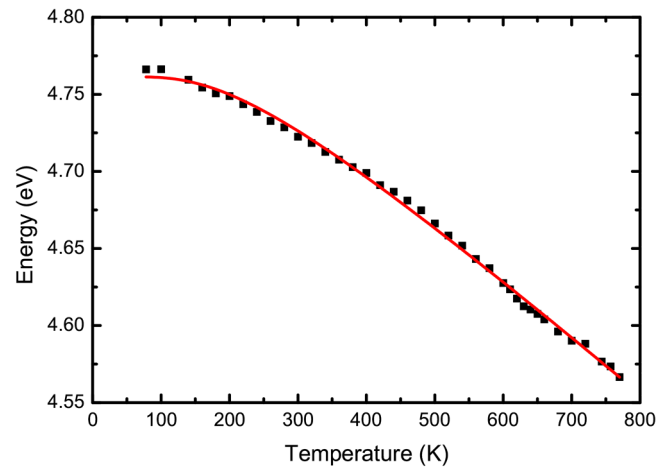

FIG. 10. Energy of the main absorption peak vs temperature. Squares: experimental data; solid line: Bose–Einstein fit with Eq. (18).

energy limits of the ellipsometry measurements as explained earlier. An important point to consider is that since the sample is kept at low temperature for a considerably long time, the formation of a very thin layer of ice or some other condensate on the surface of the sample (up to 1 nm) is inevitable. This surface condition of the sample can alter the results taken from ellipsometry measurements, whereas the electrical measurements that were employed by Farrell and Greig[38] are more likely to be insensitive to the surface conditions. The thickness of the ice layer on insulators like Ge and GaP can be specifically measured via ellipsometry.[45,46] However, the thickness of the ice on a metal cannot be measured with the same precision because metals do not have a transparent infrared spectral region.

V. MAIN PEAK AT 4.8 eV

To study the main and small peaks, we present a second set of data on the same sample and under the same measurement conditions except that the temperature step here is 10–20 K so that there are more data points available for our fitting procedure. The main peak in the optical conductivity of Ni has been assigned to $(L_2 \rightarrow L_{1u})$ based on the symmetric shape of the peak and its similarities to the main peak of gold and copper.[12] Stoll and Jung,[28] however, have assigned this peak to conduction-to-conduction band transitions. Gadenne and Lafait,[30] on the other hand, suggested that this peak can be attributed to transitions from the bottom of the d-band in different points of the Brillouin zone as it is more realistic than transitions to states well above E_F as suggested by Stoll and Jung,[28] because the density of states of Ni has a peak slightly above E_F and drops drastically with energy.

Our optical conductivity alone does not provide more information about the origin of the transition resulting in the main peak. However, the temperature dependence of the energy of this peak might shed light on the matter. Figure 10 demonstrates the red shift of the energy of this peak as the temperature rises. Shiga and Pells[12] as well as Kirillova et al.[13] report that the energy of this peak decreases linearly with temperature. However, we fit the red shift of the transition energy to the Bose–Einstein function[14]

$$E(T) = E_a - E_b \left(1 + \frac{2}{\exp(\theta/T) - 1} \right), \quad (18)$$

where $E_a = (4.88 \pm 0.01)$ eV is the unrenormalized transition energy, $E_b = (0.12 \pm 0.01)$ eV is a coupling strength, and $k\theta$ is an effective energy. We found $k\theta = (53 \pm 3)$ meV. This value is too large for an optical phonon energy, which is about 30 meV (Ref. 47) but fits the dispersion of the magnons with a normalized wave vector of approximately 0.3 from Ref. 48. The energy of the magnons can reach up to 100 meV at the L-symmetry point.[48] Therefore, the main peak appears to be due to the transitions at the L-point broadened by magnon scatterings. Neutron scattering experiments[49] show the existence of spin waves above T_c. Considering the discussion in Sec. IV, scattering by magnons results in a change in the direction of the electron (spin-flip). Furthermore, magnon assisted s-d scattering has a substantially higher probability than s-s and d-d scattering. Therefore, one can conclude that the main absorption peak of Ni is due to the transitions from the bottom of the L-point and the peak shifts as a result of the scattering by magnons.

The discrepancy between Fig. 10 and Refs. 12 and 13 appears to be due to the smaller temperature step in our experiment. Considering Fig. 10, the shift in energy for temperatures above room temperature looks linear. Both Refs. 12 and 13 conducted measurements above room temperature, and Ref. 12 has only one data point below room temperature, which was neglected in their linear fit.

Shiga and Pells[12] measured a polycrystalline Ni sample and describe the main absorption peak as a superposition of two identical peaks in the vicinity of 4.7 eV, representing the transitions of minority and majority electrons from L_2', and their energy difference of the peaks is equal to the exchange energy of the d-band ΔE_{ex}^d. They proposed that this energy difference is proportional to the reduced spontaneous magnetization (M/M_0) of Ni. They also reported this value equal to 0.46 eV, which was consistent with some theoretical calculations at the time they published their work.[50] However, later experimental band structures[51,52] showed that the exchange energy ΔE_{ex}^d is of the order of 300 meV and its magnitude and temperature dependence varies with the wave vector.[53,54] Kirillova et al.[13] conducted ellipsometry measurements on Ni(110). Their data are in good agreement with the data from polycrystalline Ni of Shiga and Pells. They further reported that the main absorption peak consists of three small peaks at room temperature and two peaks at 773 K. They concluded $\Delta E_{ex}^d = 0.25$ eV. Different values have been found for the exchange splitting of the d-band.[51,53,55,56] Stoll[27] has reported the exchange energy of the d-band of about (0.55 ± 0.07) eV from optical studies on an Ni(110) sample. However, he found this value to be 0.35 eV for polycrystalline Ni.[23] Stoll and Jung[57] estimated 0.4 eV for the exchange splitting of L_{31}. It has even been shown that the exchange splitting of the d-band has different values at different symmetry points.[56]

Our data shown in Fig. 2 demonstrate a symmetric peak and do not indicate the existence of the two peaks of Shiga and Pells, nor the three peaks of Kirillova et al.[13] Therefore, we modeled the data with only one Lorentzian oscillator at about 4.8 eV. Using two oscillators instead of one results in a high correlation between the oscillators and erroneous energies and broadenings. It also requires one oscillator with a very small amplitude compared to the other
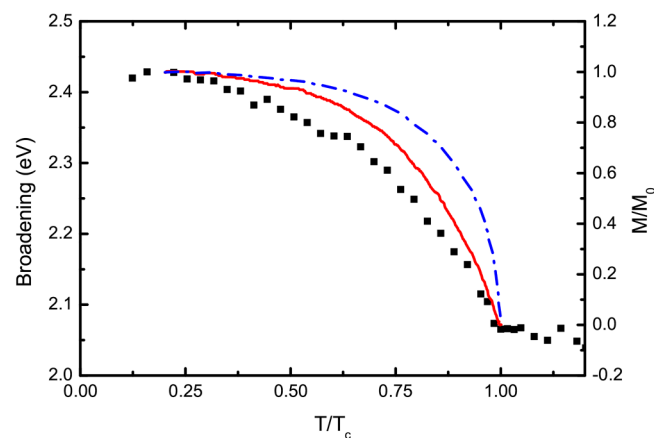
one, which is inconsistent with the model proposed by Shiga and Pells, where there are two identical oscillators.

Figure 11 shows the broadening of the main absorption peak versus temperature. The broadening starts from 2.43 eV at 77 K and reduces to 2.05 eV at 770 K. Therefore, it decreases by 0.38 eV. This reduction in broadening resembles $(M/M_0)^2$ rather than (M/M_0) proposed by Shiga and Pells.[12] As we could not fit the optical constants with two oscillators at 4.8 eV unambiguously, we believe that the reduction of the broadening of this oscillator by 0.38 eV, as opposed to the energy difference of two peaks proposed by Shiga and Pells, corresponds to ΔE_{ex}^d at the L-point, which is in agreement with the experimental value of $\Delta E_{ex}^d \approx 0.3$ eV in Refs. 51 and 55.

VI. SMALL PEAK AT 1.5 eV

Figure 2 also displays a small structure in the optical conductivity of Ni at about 1.5 eV. It has already been noticed that the separation of the contribution of the interband and intraband absorption to the conductivity of transition metals is not straightforward because a single band model with only one Drude term cannot explain the absorption.[32] While this peak at about 1.5 eV has been traditionally assigned to interband transitions at the W-point in the Brillouin zone,[12] Stoll and Jung[57] suggest assigning this peak to transitions $L_{31\uparrow} \rightarrow E_{f\uparrow}$, thus estimating an exchange splitting of $\Delta E = 0.4$ eV for L_{31}. They further conclude that the persistence of this peak at higher temperatures indicates that the exchange splitting does not reduce to zero above T_c. They previously assigned this peak to different transitions.[28]

To study the evolution of this peak as a function of temperature, in Fig. 12, we show the differential optical conductivity of the second set of data defined as $\delta\sigma_1 = \sigma_1(T) - \sigma_1(770\,\text{K})$. Considering Fig. 12, two opposite trends are apparent as one goes from temperatures above T_c (paramagnetic phase) to temperatures

FIG. 11. Broadening of the main peak at 4.8 eV (■). The solid line shows the square of the reduced spontaneous magnetization $(M/M_0)^2$ from Ref. 12. The dashed-dotted line shows the reduced spontaneous magnetization (M/M_0). The broadening of the main peak decreases with rising temperature and stays constant above T_c. The reduced magnetization is drawn to scale so the graphs coincide at the Curie temperature.
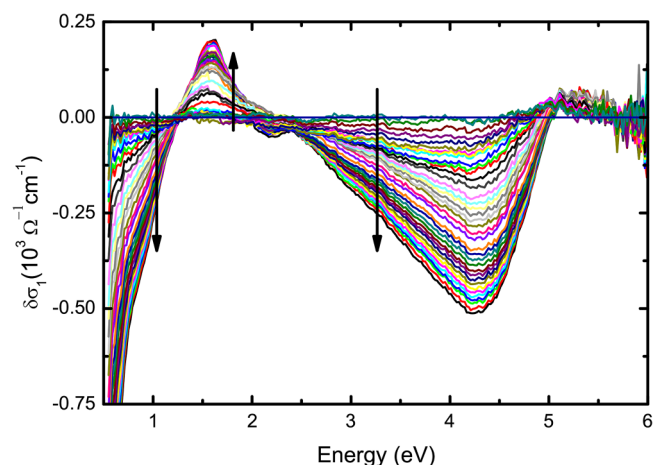

FIG. 12. Change in optical conductivity of single-crystalline Ni (100) $\delta\sigma_1 = \sigma_1(T) - \sigma_1(770\,\text{K})$ at temperatures between 77 and 770 K. The arrows show the direction of decreasing temperature from 770 to 77 K in different energy regions.
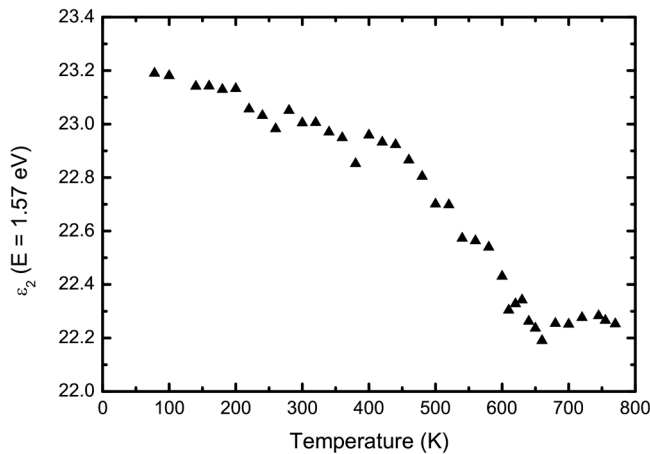
FIG. 13. Imaginary part of the dielectric function at 1.57 eV at various temperatures. ϵ_2 does not change above the Curie temperature.

FIG. 15. Proposed evolution of the minority bands ($\downarrow$) as temperature rises. (a) Ferromagnetic phase and (b) paramagnetic phase.

and is defined as[15]

$$N_{eff} = \frac{2m_0 V}{\pi \hbar e^2} \int_{E=1.23\,eV}^{E=2.00\,eV} \sigma_1(E)dE, \qquad (19)$$

where V is the volume of the unit cell and m_0 is the free electron mass. In Fig. 14, we show the change in the number of effective carriers $\delta N_{eff} = N_{eff}(T) - N_{eff}(770\,K)$ normalized by $N_{eff}(770\,K)$. This figure shows that the number of effective carriers that contribute to the absorption at the small peak stays constant in the paramagnetic phase and increases in the ferromagnetic phase as the temperature decreases. The change in the number of effective carriers in the ferromagnetic phase varies with temperature as $(M/M_0)^2$ as indicated in Fig. 14.

Considering the evolution of the small absorption peak during the transition from the ferromagnetic to the paramagnetic phase as mentioned above, we propose assigning this peak to $K_{3\downarrow} \rightarrow K_{2\downarrow}$ transitions. References 56 and 58 show that as the temperature increases, minority (majority) bands go down (up) and they coincide at T_c. Therefore, we believe that as the temperature rises the minority bands $K_{3\downarrow}$ and $K_{2\downarrow}$ move downward simultaneously, that is why the energy of the peak remains constant. This movement continues until $K_{2\downarrow}$ touches the Fermi level and stays constant at $T > T_c$. This mechanism is depicted in Fig. 15. Such a movement has been experimentally and theoretically shown for different points in the Brillouin zone.[56,58] As the bands move downward, the number of unoccupied states decreases to their minimum at T_c, which explains why the number of effective carriers decreases with rising temperature and stays constant above T_c (Fig. 14). The energy of this peak is also consistent with band structure calculation by Wang and Callaway.[59] Although our sample is single-crystalline Ni, studies on thin film Ni on Si have pointed out that the peak at about 1.5 eV becomes weaker as the crystal size becomes smaller.[30]

below T_c (ferromagnetic phase). While absorption at 4.8 eV decreases with decreasing temperature, the small absorption peak does not change down to the Curie temperature T_c and then increases with decreasing temperature below T_c. To illustrate this point, in Fig. 13 we plot the imaginary part of the dielectric function (ϵ_2) at $E = 1.57$ eV, which shows that the absorption at this energy is constant above T_c and increases below T_c with decreasing temperature. Furthermore, the energy of this peak does not show any sensitivity to the temperature, which is why we retained this energy constant in our fitting procedure.

One can calculate the effective number N_{eff} of electrons per unit cell that contribute to the conductivity of Ni in the energy range of the small peak, which comes from the sum rule
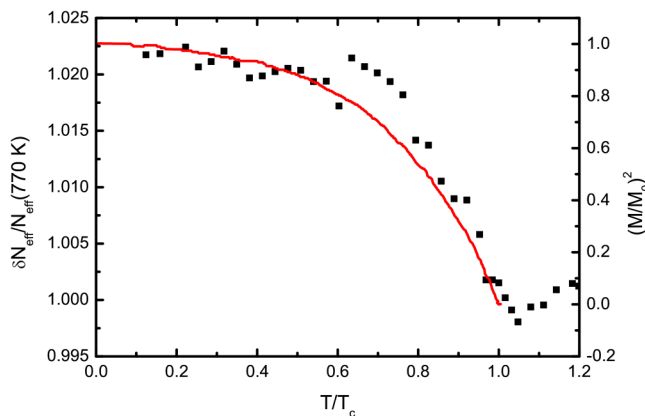

FIG. 14. Change of the effective number of carriers ($\blacksquare$) that contribute to the absorption at the small peak, normalized by the number of effective carriers at the highest temperature. The solid line shows the square of the reduced spontaneous magnetization.
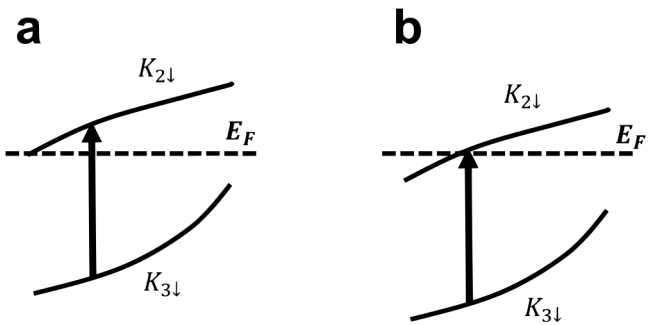
VII. SUMMARY

We modeled the optical constants of single-crystalline Ni(100) from 77 to 770 K. Qualitative agreement is found in the general shape of the resistivity from ellipsometry and electrical measurements. The temperature dependence of the resistivity is proportional

to T^2 between θ_D and T_c. The energy of the main absorption peak at 4.8 eV displays a red shift upon rising temperature, which is modeled by a Bose–Einstein function. The fit gives an effective scattering energy of about 53 meV for these transitions, which we interpret as an interband transition scattered by magnons. The broadening of the main peak reduces by 0.38 eV and stays constant above T_c. Therefore, the reduction of the broadening of this peak is interpreted as ΔE_{ex}^d at the L-point. The temperature dependence of the small absorption peak at 1.5 eV is explained by assigning it to the $K_{3\downarrow} \rightarrow K_{2\downarrow}$ transition, which explains the decrease in magnitude of the peak and its constant energy. We have conducted the same set of measurements on a polycrystalline Ni sample and observed the same changes in its optical properties. Therefore, our results are expected to be applicable not only to Ni (100) but also to Ni (111) and other orientations.

ACKNOWLEDGEMENT

AUTHOR DECLARATIONS

Conflict of Interest

The authors have no conflicts to disclose.

Ethics Approval

Ethics approval is not required.

DATA AVAILABILITY

The data that support the findings of this study are available from the corresponding author upon reasonable request.

REFERENCES

[1]F. Abadizaman and S. Zollner, J. Vac. Sci. Technol. B 37, 062920 (2019).
[2]N. F. Mott, Proc. R. Soc. A 167, 580 (1938).
[3]J. C. Slater, Phys. Rev. 36, 57 (1930).
[4]J. C. Slater, Phys. Rev. 49, 537 (1936).
[5]A. H. Wilson, Proc. R. Soc. A 153, 699 (1936).
[6]W. G. Baber, Proc. R. Soc. A 158, 383 (1937).
[7]C. S. Wang and J. Callaway, Phys. Rev. B 9, 4897 (1974).
[8]W. Nolting, W. Borgiel, V. Dose, and T. Fauster, Phys. Rev. B 40, 5015 (1989).
[9]W. Borgiel and W. Nolting, Z. Phys. B Condens. Matter 78, 241 (1989).
[10]M. J. Laubitz, T. Matsumura, and P. J. Kelly, Can. J. Phys. 54, 92 (1976).
[11]R. C. O'Handley, Modern Magnetic Materials: Principles and Applications (Wiley, New York, 2000).
[12]M. Shiga and G. P. Pells, J. Phys. C: Solid State Phys. 2, 1847 (1969).
[13]M. M. Kirillova, Y. V. Knyavez, and Y. I. Kuzmin, Thin Solid Films 234, 527 (1993).
[14]L. Viña, S. Logothetidis, and M. Cardona, Phys. Rev. B 30, 1979 (1984).
[15]P. Friš, D. Munzar, O. Caha, and A. Dubroka, Phys. Rev. B 97, 045137 (2018).
[16]MTI Corporation, 860 S. 19th Street, Richmond, CA 94804, USA.
[17]F. Abadizaman, "Optical characterization of Ni using spectroscopic ellipsometry at temperatures from 80 K to 780 K," Doctoral dissertation (New Mexico State University, ProQuest Dissertation Publishing 2020) (Accession No. 28156132).
[18]S. Zollner, F. Abadizaman, C. Emminger, and N. Samarasingha, "Spectroscopic ellipsometry from 10 to 700 K," Adv. Opt. Techn. (Submitted).
[19]H. Fujiwara, Spectroscopic Ellipsometry (Wiley, Chichester, 2007).
[20]S. Roberts, Phys. Rev. 114, 104 (1959).
[21]P. Drude, Physik. Z. 1, 161 (1900).
[22]P. Drude, The Theory of Optics (Longmans, Green, and Company, New York, 1902), p. 398.
[23]M. P. Stoll, Solid State Commun. 8, 1207 (1970).
[24]H. Ehrenreich, H. R. Philipp, and D. J. Dlechna, Phys. Rev. 131, 2469 (1963).
[25]D. G. Laurent and J. Callaway, Phys. Rev. B 20, 1134 (1979).
[26]P. B. Johnson and R. W. Christy, Phys. Rev. B 11, 1315 (1975).
[27]M. P. Stoll, J. Appl. Phys. 42, 1717 (1971).
[28]M. P. Stoll and C. Jung, J. Phys. F: Metal Phys. 9, 2491 (1979).
[29]S. Zollner, P. P. Paradis, F. Abadizaman, and N. S. Samarasingha, J. Vac. Sci. Technol. B 37, 012904 (2019).
[30]M. Gadenne and J. Lafait, J. Phys. France 47, 1405 (1986).
[31]H. Ibach and S. Lehwald, Solid State Commun. 45, 633 (1983).
[32]H. M. Kirillova, Sov. Phys. JETP 34, 178 (1972) [Zh. Eksp. Teor. Fiz. 61, 336 (1971)].
[33]B. Raquet, M. Viret, E. Sondergard, O. Cespedes, and R. Mamy, Phys. Rev. B 66, 024433 (2002).
[34]N. V. Volkenshtein, V. P. Dyakona, and V. E. Startsev, Phys. Status Solidi B 57, 9 (1973).
[35]G. K. White and S. B. Woods, Philos. Trans. R. Soc. A 251, 273 (1959).
[36]C. Y. Ho, W. Powell, and P. E. Liley, J. Phys. Chem. Ref. Data 3, 1 (1974).
[37]G. R. Stewart, Rev. Sci. Instrum. 54, 1 (1983).
[38]T. Farrell and D. Greig, J. Phys. C: Solid State Phys. 1, 1359 (1968).
[39]D. A. Goodings, Phys. Rev. 132, 542 (1963).
[40]B. Raquet, M. Viret, J. M. Broto, E. Sondergard, O. Cespedes, and R. Mamy, J. Appl. Phys. 91, 8129 (2002).
[41]I. A. Campbell and A. Fert, Ferromagnetic Materials, edited by E. P. Wohlfarth (North Holland, Amsterdam, 1982), Vol. 3, p. 747.
[42]T. Kasuya, Prog. Theor. Phys. 16, 58 (1956).
[43]S. V. Vonsovskii and Y. A. Izyumov, Usp. Fiz. Nauk. 77, 377 (1962).
[44]M. W. Stringfellow, J. Phys. C: Solid State Phys. 1, 950 (1968).
[45]C. Emminger, F. Abadizaman, N. S. Samarasingha, T. E. Tiwald, and S. Zollner, J. Vac. Sci. Technol. B 38, 012202 (2020).
[46]N. S. Samarasingha and S. Zollner, J. Vac. Sci. Technol. B 39, 052201 (2021).
[47]Q. Bian, S. K. Bose, and R. S. Shukla, J. Phys. Chem. Solids 69, 168 (2008).
[48]E. D. Thompson and J. J. Myers, Phys. Rev. 153, 574 (1967).
[49]G. Shirane, O. Steinsvoll, Y. J. Uemura, and J. Wicksted, J. Appl. Phys. 55, 1887 (1984).
[50]S. Wakoh, J. Phys. Soc. Jpn. 20, 1894 (1965).
[51]D. E. Eastman, F. J. Himpsel, and J. A. Knapp, Phys. Rev. Lett. 40, 1514 (1978).
[52]T. J. Kreutz and T. Greber, Phys. Rev. B 58, 1300 (1998).
[53]K. P. Kämper, W. Schmitt, and G. Güntherodt, Phys. Rev. B 42, 10696 (1990).
[54]R. Raue and H. Hopster, Z. Phys. B Condens. Matter 54, 121 (1984).
[55]F. J. Himpsel, J. A. Knapp, and D. E. Eastman, Phys. Rev. B 19, 2919 (1979).
[56]W. Borgiel, W. Nolting, and M. Donath, Solid State Commun. 72, 825 (1989).
[57]M. P. Stoll and C. Jung, J. Appl. Phys. 50, 7477 (1979).
[58]T. Greber, T. J. Kreutz, and J. Osterwalder, Phys. Rev. Lett. 79, 4465 (1997).
[59]C. S. Wang and J. Callaway, Phys. Rev. B 15, 298 (1977).